Resonance Averaged Photoionization Cross Sections for Astrophysical Models

Manuel A. Bautista

Laboratory for High Energy Astrophysics, Code 662

NASA Goddard Space Flight Center, Greenbelt, MD 20771

Patrizia Romano, & Anil K. Pradhan

Department of Astronomy, The Ohio State University

174 West 18th Avenue, Columbus, OH 43210-1106

ABSTRACT

We present ground state photoionization cross sections of atoms and ions averaged over resonance structures for photoionization modeling of astrophysical sources. The detailed cross sections calculated in the close-coupling approximation using the R-matrix method, with resonances delineated at thousands of energies, are taken from the Opacity Project database TOPbase and the Iron Project, including new data for the low ionization stages of iron Fe I – V. The resonance-averaged cross sections are obtained by convolving the detailed cross sections with a Gaussian distribution over the autoionizing resonances. This procedure is expected to minimize errors in the derived ionization rates that could result from small uncertainties in computed positions of resonances, while preserving the overall resonant contribution to the cross sections in the important near threshold regions. The detailed photoionization cross sections at low photon energies are complemented by new relativistic distorted-wave calculations for $Z \leq 12$, and from central-field calculations for $Z > 12$ at high energies, including inner-shell ionization. The effective cross sections are then represented by a small number of points that can be readily interpolated linearly for practical applications; a Fortran subroutine and data are available. The present numerically averaged cross sections are compared with analytic fits that do not accurately represent the effective cross sections in regions dominated by resonances.

Subject headings: atomic data – atomic processes

1. Introduction

Photoionization cross sections are necessary for the computation of photoionization and recombination rates for ionization balance in astrophysical plasmas (e.g. Kallman and Krolik 1991, Shull & Van Steenberg 1982, Sutherland & Dopita 1993). Accurate cross sections have been calculated in the close-coupling approximation using the R-matrix method, for most astrophysically important atoms and ions under the Opacity Project (OP; Seaton et al. 1994) and the Iron Project (IP; Hummer et al. 1993). The cross sections incorporate, in an *ab initio* manner, the complex autoionizing resonance structures that can make important contributions to total photoionization rates. These data are currently available from the electronic database of the Opacity Project TOPbase (Cunto et al. 1993; *The Opacity Project Team* 1995).

Resonant phenomena have been shown to be of crucial, often dominant, importance in electron-ion scattering, photoionization, and recombination processes (see, for example, the references for the OP and the IP). Most of the related calculations for such atomic processes have been carried out in the close-coupling (hereafter CC) approximation that quantum mechanically couples the open and closed channels responsible for the continuum, and the quasi-bound resonant states, respectively. Photoionization calculations in the CC approximation consist of an expansion over the states of the (e + ion) system, with a number of excited states of the residual (photoionized) ion (also called the "target"). The CC approximation thereby includes, in an *ab initio* manner, several infinite Rydberg series of resonances converging on to the states of the target ion. The resonances are particularly prominent in the near-threshold region due to strong electron correlation effects, and the accuracy of the calculated cross section depends on the representation of the resonances. Furthermore, singular resonant features may sometimes dominate the cross section over an extended energy region. A prime example of such resonances, in addition to

the Rydberg series of resonances and the broad near-threshold resonances, are the so called "photoexcitation-of-core" (PEC) resonances that occur at higher energies corresponding to photoexcitation of dipole transitions in the residual ion by the incident photon (Yu & Seaton 1987). The PECs are very large features that attenuate the background cross section by up to orders of magnitude, and are present in many of the cross sections in all ions with target states coupled by dipole transitions, i.e., even and odd parity LS terms. Much of the effort in the decade-long Opacity Project was devoted to a careful consideration and delineation of resonances using the R-matrix method which has the advantage that once the (e + ion) Hamiltonian has been diagonalized in the R-matrix basis, cross sections may be computed at an arbitrary number of energies to study resonant phenomena. The methods and a number of calculations are described in the volume *The Opacity Project* by the Opacity Project Team (1995).

Owing to the complexity in the structure of the cross sections, thousands of points are normally calculated to represent the detailed cross sections for each bound state of an ion or atom. While this is a great advance in terms of atomic physics and accuracy, the huge amount and the inherent details of the data do present a serious practical problem for numerical modeling. An additional difficulty in the use of these cross sections for photoionization modeling is uncertainty in the precise positions of these resonances. The OP cross sections were calculated primarily for the computation of Rosseland and Planck mean opacities in local thermodynamic equilibrium (LTE) for stellar envelope models (Seaton et al. 1994); the cross sections at all photon frequencies are integrated over the Planckian black-body radiation field. Whereas the LTE mean opacities are insensitive to small uncertainties in the precise locations of resonances in photoionization cross sections, the situation is different for the calculation of photoionization rates of individual atomic species in non-LTE astrophysical sources photoionized by radiation fields that include spectral lines, such as H II regions or active galactic nuclei (AGN). There may be spurious

coincidences between the strong lines and the narrow resonance features in the original data. On the other hand, the physical presence of extensive structures of resonances in cross sections has a pronounced effect on the total photoionization rate that should not be neglected, as exemplified by recent work on Fe ions (Nahar, Bautista, & Pradhan 1997a, Bautista & Pradhan 1998). Thus, a numerical procedure is needed that accurately and efficiently reproduces the new CC cross sections for astrophysical modeling, in particular the extensive OP photoionization cross section data in TOPbase.

In some previous works analytic fits have been presented for partial photoionization cross sections of sub-shells (Verner et al. 1993, Verner and Yakovlev 1995), and for the OP cross sections "smoothed" over resonances (Verner et al. 1996). However, analytic fits can not reproduce the well localized effects of resonances and groups of resonances. In their approach, Verner et al. (1996) smoothed over resonances at variable energy intervals whose widths were adjusted until the resonance structures disappeared. In some cases, however, very large resonances could not be smoothed, so they were neglected in the fits. The analytic fits of Verner et al. seem computationally efficient for modeling computer codes. However, the smoothing procedure is unphysical and artificially deletes most of the extensive resonance structures in the OP cross sections. In addition, as we show later, neglecting very large resonances results in errors in the fitted cross sections and in the resulting photoionization rates. Although such errors in the photoionization rates are difficult to quantify in general, due to the frequency dependence of the irregular radiation field that varies from object to object and from one point to another within the same object, we present several quantitative estimates for specific cases.

In this paper we compute resonance-averaged photoionization (RAP) cross sections from a convolution with a running Gaussian distribution over energy intervals that subsume the uncertainties in resonance positions, estimated to be about 1% from a comparison of

the calculated bound state energy levels with spectroscopic measurements (*The Opacity Project Team*, 1995). This procedure should minimize errors in ionization rates due to inaccuracies in resonance positions, while taking into account their contributions and preserving the overall physical complexities in the structure of the cross sections, especially in the important near threshold region. Further, RAP cross sections effectively simulate some broadening processes, notably thermal (Doppler) broadening, that result in a natural smearing of the sharp resonance features. Thus, RAP cross sections assume a qualitatively physical form even though the quantitative aspects may not be generalized for all sources.

The differences between photoionization rates calculated with the present RAP cross sections, and the detailed cross sections, are studied for a variety of radiation fields. The relatively low-energy cross sections from the OP and IP are merged with cross sections from Relativistic Distorted Wave calculations by Zhang (1997) for high photon energies including inner-shell ionization from closed sub-shells (not considered in the OP data), and from the Hartree-Slater central-field calculations by Reilman & Manson (1979). Further, we employ a numerical technique for representing the photoionization cross sections by a small number of points, from the photoionization threshold to very high energies. The tabulated cross sections can be readily coded in computer modeling programs to enable accurate computation of photoionization rates for an arbitrary ionizing radiation flux. A Fortran subroutine RESPHOT is made available to users to facilitate the interface of RAP data with models.

2. Resonance-Averaged Photoionization (RAP) Cross Sections

The uncertainty in the position of any given feature in the photoionization cross section may be represented by a probabilistic Gaussian distribution of width δE around the position predicted by the theoretical calculation. There is, in principle, no reason to expect

that the accuracy should vary with the central energy of a given feature or from one cross section to another. Thus we can assume $\delta E/E \equiv \Delta$ to be constant. Then the averaged photoionization cross section in terms of the detailed theoretical cross section convolved over the probabilistic distribution is

$$\sigma_A(E) = C \int_{E_0}^{\infty} \sigma(x) \, \exp\left[-(x-E)^2/2(\delta E)^2\right] \, dx, \tag{1}$$

where σ and σ_A are the detailed and averaged photoionization cross sections respectively, E_o is the ionization threshold energy, and C is a normalizing constant.

Fig. 1 compares the detailed and the RAP cross sections for Fe II (Nahar & Pradhan 1994) and Fe I (Bautista 1997) for choices of the $\Delta = 0.01, 0.03, 0.05,$ and 0.10. The convolved cross sections with the Gaussian distribution are smooth even across regions of intricate resonance structures. In regions free of resonances the RAP cross sections asymptotically approach the original cross sections without loss of accuracy. It is observed that the choice of the width of the Gaussian distribution has an appreciable effect on the resulting RAPs. As the width of the distribution decreases the RAPs show more structure resembling the detailed resonant structure. On the other hand, if the chosen width of the distribution is too large the overall structure of the cross sections in the resonant region is smeared over and the background may be unduly altered. This is seen in the case of Fe II (Fig. 1(a)) and Fe I (Fig.1(b)) in the 0.8 to 0.9 Ry region that lies between large resonance structures.

Based on such numerical tests, we adopt a standard width for all the cross sections of $\Delta = 0.03$ (solid lines in Fig. 1(a) and (b)). This choice is sufficiently conservative with respect to the uncertainties in the theoretical cross sections and is able to provide RAP cross sections that resemble reasonably well the overall structure of the cross sections. This choice of Δ also yields RAPs sufficiently smooth to be represented by small number of points that lead to accurate photoionization rates ((see Sections 4 and 5).

3.   The Data

The OP ground state photoionization cross sections for atoms and ions of He through Si (Z = 2 – 14), and S, Ar, Ca, and Fe are obtained from TOPbase (Cunto et al. 1993). For the lowest ionization stages of Iron, Fe I – V, radiative data of much higher accuracy than those from the OP have recently been computed under the IP (Table 1 of Bautista & Pradhan 1998) and have been included in the present work (detailed references are given in the Appendix). The R-matrix calculations performed under the OP and IP were carried out for photon energies up to just above the highest target state in the CC expansion for the residual core ion. The first version of TOPbase included OP cross sections with power law tails extrapolated to energies higher than in the R-matrix calculations. High energy cross sections, however, have now been calculated for all the ground and excited states of atoms and ions with Z≤ 12 using a fully relativistic distorted-wave method (Zhang 1997) that includes the inner-shell 'edges' not considered in the original OP data. The low energy R-matrix cross sections smoothly match the high energy distorted-wave tails; which yields a consistent set of merged (OP + RDW) results that should be accurate for all energies of practical interest. For the lowest ionization stages of S, Ar, Ca, and Fe that are not included in Zhang's calculations, we have adopted central-field high energy cross sections by Reilman & Manson (1979).

4.   Numerical Representation of the RAP Cross Sections

Having calculated the RAP cross sections, we represent these with a minimum number of points selected so that the cross section can be recovered by linear interpolation to an accuracy better than 3%. We obtain a representation for the cross sections, from the ionization threshold to very high photon energies including all of the inner shell ionization edges, with approximately 30 points per cross section. Examples of the RAP cross sections,

and differences with the analytic fits (Verner et al. 1996), are illustrated in Fig. 2 for S I and Fe I. It is clear that for these two important elements these differences are substantial and would correspondingly affect the photoionization rates. In particular it may be noted that the effect of resonances varies significantly with energy, representative of the complex atomic effects such as the Rydberg series limits that can not be reproduced by any analytic procedure. For example, the resonance- averaged structure in the RAP cross section for S I in the near-threshold region is a rise and a dip, corresponding to actual resonances. The resonances make an even greater contribution for Fe I and the analytic fit is likely to yield a serious underestimation of the photoionization of neutral iron.

Fig. 3 presents RAP cross sections for several other elements, with some singularly large features over wide energy ranges (e.g. Fe IV and Al I). Keeping in mind the 1% or so uncertainty in the resonance positions, the RAPs represent these physical features (an extensive discussion of the resonant feature in Fe IV is given by Bautista & Pradhan 1997). Fig. 3 also show the discrete sets of points that can be interpolated for a detailed and accurate representation of the averaged cross sections. Such a representation is not possible with analytic fits. In addition to a more accurate representation of the atomic physics the present RAP cross sections should also be computationally preferable to analytic fits since a single set of points can reproduce the effective cross section, while analytic fits require several formulae and parameters for all of the inner-shell contributions.

5.   Accuracy of RAP Cross Sections

A careful study of the accuracy of the RAP cross sections and their reduced representation is important if they are to be used for practical applications. Any reasonable transformation or smoothing procedure of the photoionization cross sections should conserve the total area under the cross section function integrated over a certain energy integral.

This, however, gives no indication about the actual accuracy of the transformed function. A good indication of the uncertainty in the cross sections may be obtained from the photoionization rates that result from the product of the cross section and a radiation field integrated over the photon energy from the ionization threshold to infinity. The radiation fields in practice are complicated functions of frequency and may even vary from one point to another within the same object, as well as from object to object. Then, different radiation field functions would sample preferentially distinct energy intervals in the cross sections and may be used as an accuracy indicator.

For the present work we have selected nine different ionizing radiation fields that are expected to represent some general conditions for a number of cases of astrophysical interest. These radiation fields correspond to ionizing sources typical of an O star with T_{eff}= 40,000 K, a high luminosity star with T_{eff}= 100,000 K, and an extremely hot $T = 10^8$ K black body source. Each of these sources is assumed to be surrounded by a gaseous envelope with nearly cosmic chemical composition under pressure equilibrium conditions. The densities of the ionized gas at the near side to the source are taken to be 10^4, 3×10^3, and 10^{10} cm^{-3}, respectively. Under photoionization equilibrium the physical parameters were calculated for each of these nebulae using the computer code CLOUDY (Ferland 1993), and three different ionizing radiation fields were obtained for each case corresponding to the conditions at the near side of the cloud, at half depth of the ionized cloud, and near the ionization front. As an example, the radiation fields selected for the T_{eff}= 100,000 K source are shown in Fig. 4.

All detailed OP cross sections, their RAP cross sections, and their reduced representations (linearly interpolated values between the RAP cross sections), were integrated over the different radiation fields to obtain the photoionization rates and the results compared. Photoionization rates obtained with detailed cross sections and RAP

cross sections agree within 5%.

When comparing the photoionization rates with those obtained from the analytic fits of Verner et al. (1996), significant differences are found. The most prominent differences are for the lower ionization stages of iron Fe I – V, and Na VII, for which the fits of Verner et al. give photoionization rates differing by up to about 70%. Differences between 20-30% are found for Be I, S IV, Ar II, Fe VII, and Fe XI, and between 10-20% for B I, S VII, Mg I, Mg II, Al I, Ar I, Ar III, Ar V, and Fe VIII. For all other ions the fits of Verner et al. yield photoionization rates that agree to within 10% with the present results. This agreement for the last set of data is primarily for the multiply ionized systems where the resonances are usually narrow and the resonance contributions, relative to the background, are small. It is emphasized that the errors in the photoionization rates when using analytic fits for the cross sections vary with the shape of the radiation field and are unpredictable in general.

6.   Recombination Rates and Ionization Fractions

A further check on the new RAP cross sections may be made by computing ionization fractions in photoionization equilibrium. These calculations also require (electron-ion) recombination rate coefficients. In recent years a unified method has been developed that incorporates radiative and dielectronic recombination (RR and DR) in an *ab initio* manner, and enables the calculation of total (e + ion) recombination rates in the CC approximation using the R-matrix method (Nahar & Pradhan 1992, 1995). In addition, the new recombination rates are fully self-consistent with the photoionization cross sections as both the photoionization and the recombination data are calculated in the CC approximation using the same eigenfunction expansion over the states of the residual ion. Unified, total recombination rates have been computed so far for approximately 33 atoms and ions, including all C, N, O ions (Nahar and Pradhan 1997, Nahar 1998), the C-sequence

ions (Nahar 1995,1996), and Fe ions Fe I – V (references are given in Bautista & Pradhan 1998).

In a recent work on iron emission and ionization structure in gaseous nebulae (Bautista & Pradhan 1998) the new photoionization/recombination data for Fe I – V, including detailed and RAP cross sections, was employed to obtain ionic fractions of Fe in a photoionized H II region (the Orion nebula), and considerable differences were found with previous works. In this work we compute a few C, N, O ionization fractions using the RAP cross sections computed in the present work and the new unified (e + ion) recombination rates, to study the effect of the new photoionization/recombination data. Although the differences for lighter elements are relatively smaller than for the Fe ions, they can be significant in temperature ranges in transition regions between adjacent ionization stages, as illustrated in Fig. 5. Whereas there is no significant difference in the RAP cross sections computed in this work for C,N, and O, and the earlier ground state photoionization data incorporated in CLOUDY, some significant differences are found when the new unified recombination data for C,N,O ions is employed.

7.   FORTRAN Subroutines and Data

The RAP cross sections for the ground state of all atoms and ions in TOPbase, and new data for Fe I – V and some other ions, are available in a FORTRAN subroutine RESPHOT that can be readily interfaced with modeling codes. The routine is available electronically from the authors. Given an ion stage (N,Z) and an energy in Rydbergs, RESPHOT returns the linearly interpolated value of the photoionization cross section from the table of points described in Section 4. It is also important to point out that the RAP cross sections are given as a function of the energy of the ejected electron (i.e., energies with respect to the ionization threshold) instead of the photon energies in TOPbase that are relative to the

first ionization potential calculated to about 1% accuracy. Users can easily scale the cross sections to the more accurate experimental ionization potentials.

Also available is a routine RCRATE which gives total unified e-ion recombination rates that may be used instead of the combination of previously available (and often inaccurate) data on RR and DR rates. Given an ion stage (N,Z) and an electron temperature, RCRATE returns the total recombination rate coefficient interpolated from the tables of Nahar (1995,1996), Nahar and Pradhan (1997), and the references in Table 1 of Bautista and Pradhan (1998).

RESPHOT and RCRATE can be easily interfaced with photoionization codes such CLOUDY, as demonstrated by their use to produce the results in Figs. 4 and 5.

8.   Conclusion

Resonance-averaged photoionization (RAP) cross sections have been calculated for most atoms and ions of astrophysical importance using the Opacity Project data from TOPbase and new data on Fe and C,N,O ions. These incorporate the effect of autoionizing resonances in an averaged manner that is not too sensitive to the precise positions of resonances, but accounts for the often significant attenuation of the effective cross sections that is neglected in earlier works. The RAP cross sections have been represented by a small number of points that can be readily interpolated in modeling codes to reproduce photoionization cross sections at all energies of practical interest, including inner-shell ionization thresholds. Illustrative examples show considerable differences with analytic fits that neglect resonance structures. It is also pointed out that new recombination rates, unifying the radiative and dielectronic recombination processes, are being computed for astrophysically abundant elements to provide a self-consistent set of photoionization/recombination data for modeling

astrophysical sources in radiative equilibrium.

Appendix

Table 1.   References to the Photoionization Cross Sections

Ion	Reference
He-like	Fernley et al. 1987
Li-like	Peach et al. 1988
Be-like	Tully et al. 1990
B I	Berrington & Hibbert, in preparation
B-like	Fernley et al., in preparation
C-like	Luo & Pradhan 1989
N-like	Burke & Lennon, in preparation
O-like, F-like	Butler & Zeippen, in preparation
Ne-like	Scott, in preparation
Na-like	Taylor, in preparation
Mg-like	Butler et al. 1993
Al-like	Mendoza et al. 1995
Si-like	Nahar & Pradhan 1993
P-like	Butler et al., in preparation
S-like	Berrington et al., in preparation
Cl-like	Storey & Taylor, in preparation
Fe IX	Butler et al., in preparation
Ar-like	Saraph & Storey, in preparation

Table 1—Continued

Ion	Reference
Fe VIII	Butler et al. , in preparation
Fe VII	Sawey & Berrington 1992
Ca-like	Saraph & Storey, in preparation
Fe VI	Butler et al., in preparation
Fe V	Bautista 1996
Fe IV	Bautista & Pradhan 1997
Fe III	Nahar 1996
Fe II	Nahar & Pradhan 1994
Fe I	Bautista 1997

REFERENCES

Bautista, M.A. 1996, A&AS, 119, 105

— 1997, A&AS, 122, 167

Bautista, M.A. & Pradhan, A.K. 1997, A&AS(in press)

— 1998, ApJ(in press)

Butler, K., Mendoza, C., & Zeippen, C. J. 1993, J. Phys. B, 26, 4409

Butler, K., Zeippen, C.Z. 1990, A&A, 234, 569

Cunto, W., Mendoza, C., Ochsenbein, F., & Zeippen, C.J. 1993, A&A, 275, L5

Ferland, G.J. 1993, University of Kentucky Department of Physics and Astronomy Internal Report (CLOUDY)

Fernley, J. A., Taylor K. T. & Seaton, M. J. 1987, J. Phys. B, 20, 6457

Hummer, D.G., Berrington, K. A., Eissner, W., Pradhan, A. K., Saraph, H. E., & Tully, J. A. 1993, A&A, 279, 298

Kallman, T. R., and Krolik, J. H., 1991, GSFC Special Report

Luo, D., & Pradhan, A. K. 1989, J. Phys. B, 22, 3377

Mendoza, C., Eissner, W., Le Dourneuf, M., & Zeippen, C. J. 1995, J. Phys. B, 28, 3485

Nahar, S.N. 1995, ApJS, 101, 42

— 1996, ApJS, 106, 213

— 1998, ApJS (submitted)

Nahar, S.N., Bautista. M.A., & Pradhan, A.K. 1997a, ApJ, 479, 497

Nahar, S.N., and Pradhan, A.K. 1992, Phys. Rev. Lett., 68, 1488

— 1994, Phys. Rev. A, 46, 1916

— 1995, ApJ, 447, 966

— 1997, ApJS, 111,339

Peach, G., Saraph, H. E., & Seaton, M. J. 1988, J. Phys. B, 21, 3669

Reilman, R.F. & Manson, S.T. 1979, ApJS, 40, 815

Sawey, P. M. J., & Berrington, K. A. 1992, J. Phys. B, 25, 1451

Seaton, M.J., Yu Yan, Mihalas, D., & Pradhan, A.K. 1994, MNRAS, 266, 805

Shull, J.M., & Van Steenberg, M. 1982, ApJS, 48, 95; ApJS, 49,351

Sutherland, R.A. & Dopita, M.A. 1993, ApJS, 88, 253

The Opacity Project Team 1995, *The Opacity Project*, Institute of Physics Publishing, Bristol UK

Tully, J. A., Seaton M. J., & Berrington, K. A. 1990, J. Phys. B, 23, 3811

Verner, D.A., Ferland, G.J., Korista, K.T., & Yakovlev, D.G. 1996, ApJ, 465, 487

Verner, D.A. & Yakovlev, D.G. 1995, A&AS, 109. 125

Verner, D. A., Yakovlev, D. G., Brand, I. M., Trzhaskovskaya, M. B. 1993, At. Data Nucl. Data Tab. 55, 233

Yu Yan & Seaton, M.J. 1987, J. Phys. B: At. Opt. Phys., 20,6409
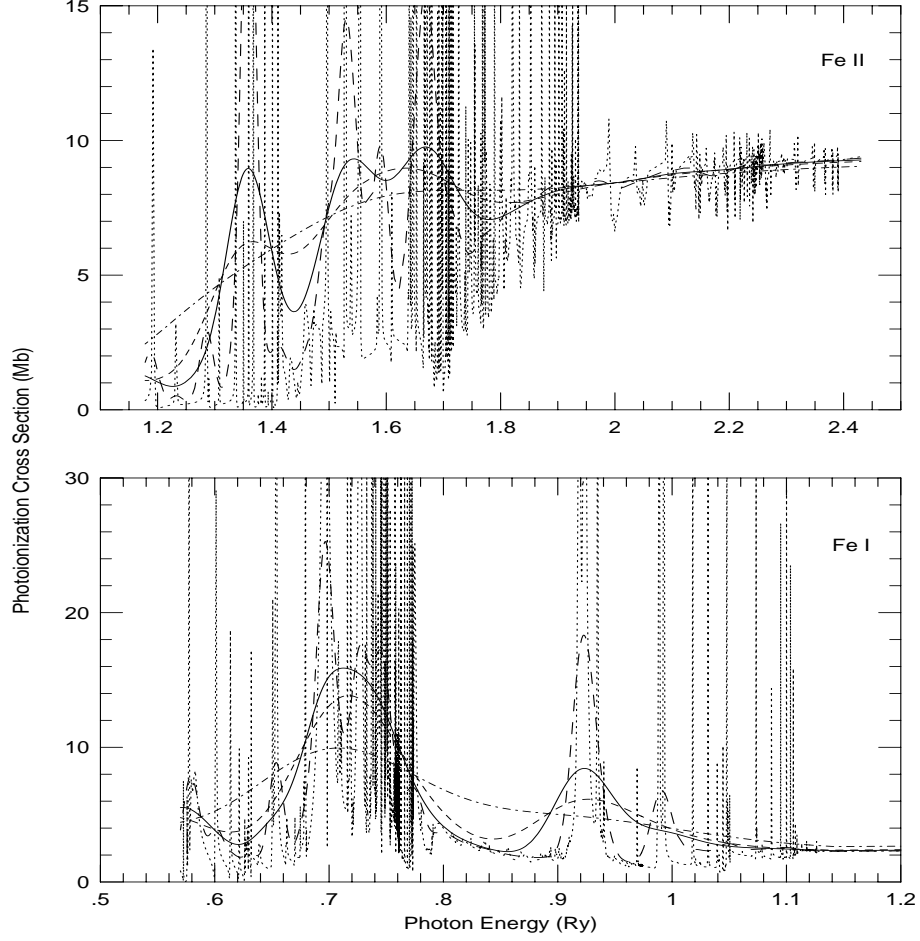
Zhang, H.L. 1997, A&AS, submitted

Fig. 1.— Ground state photoionization cross sections for Fe^+ (a) and Fe^0 (b). The detailed cross sections are shown by the dotted line and the resonance-averaged cross sections are shown for $\delta E/E = 0.01$ (long dashed line), 0.03 (solid line); 0.05 (short dashed line), and 0.10 (dot-dashed line).
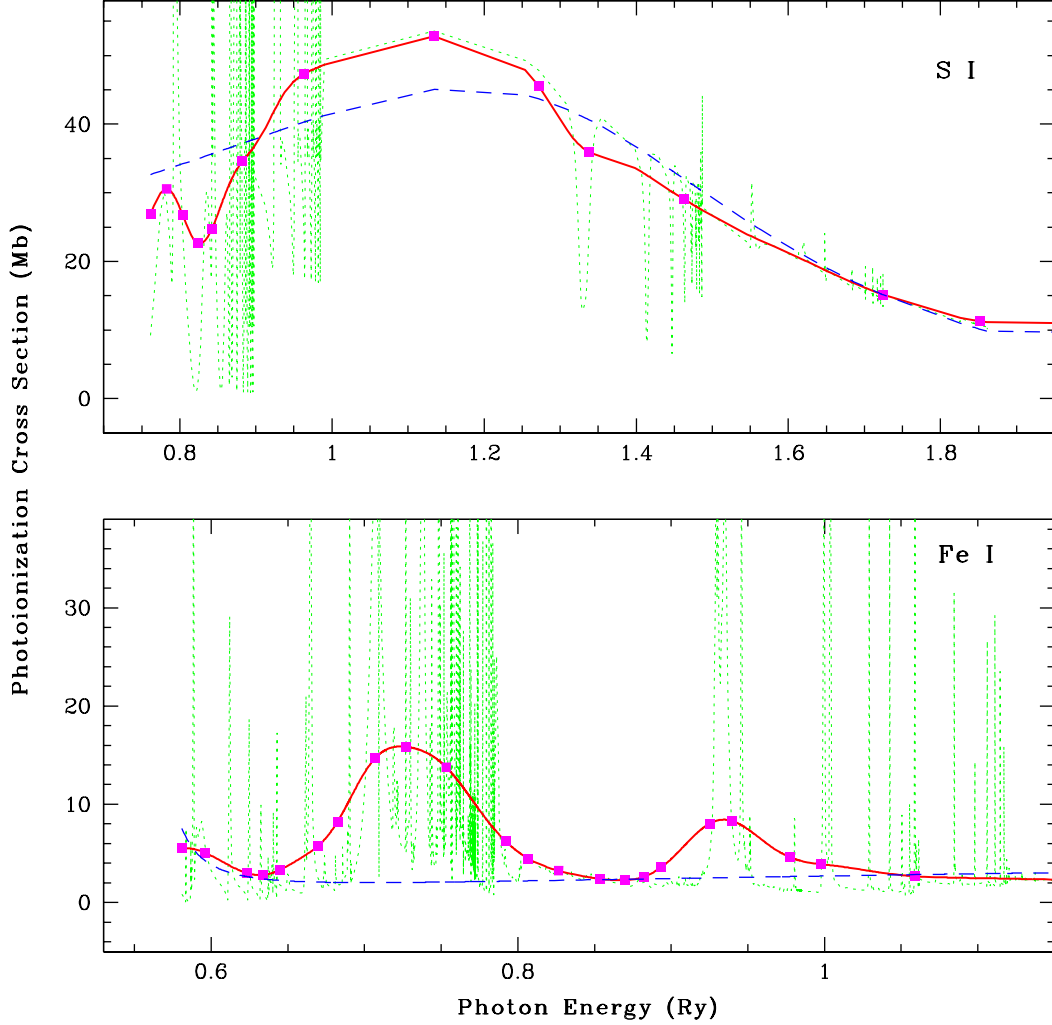
Fig. 2.— Sample of resonance-averaged photoionization (RAP) cross sections (solid line) for S I and Fe I; filled squares are points chosen to represent the RAP cross sections. The short-dashed line is the detailed OP cross section, the long-dashed line is the cross section from analytic fits by Verner et al. (1996).
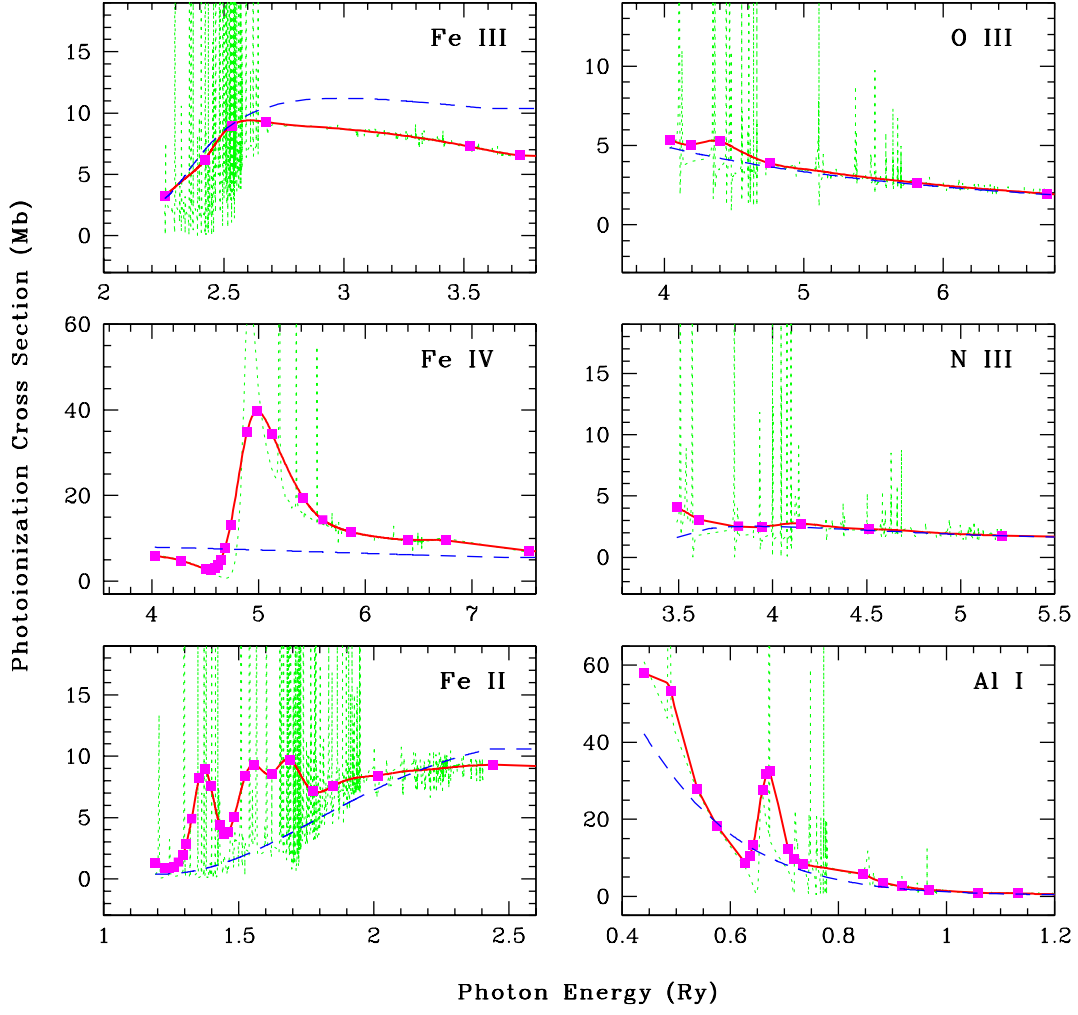
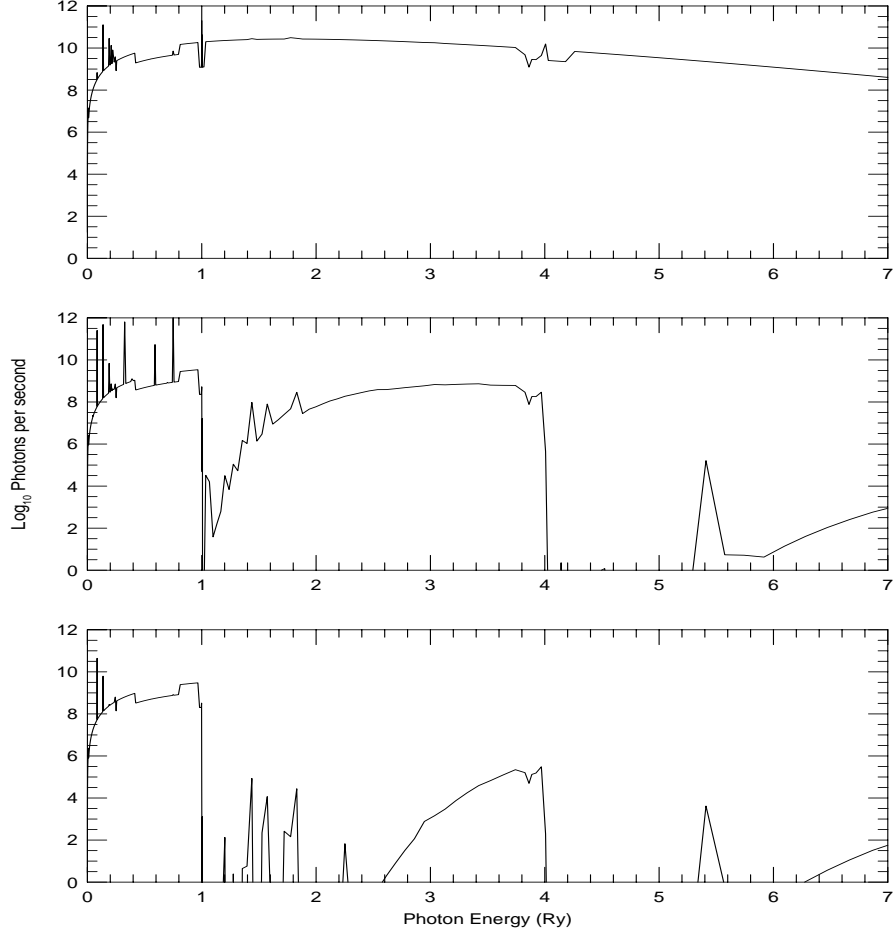Fig. 3.— Sample of RAP cross sections for several other ions (as in Fig. 2).

Fig. 4.— Sample of ionizing radiation fields at different points in a photoionized nebula. The radiation fields shown are those at the near side of the cloud, at half depth, and near the ionization front, (top to bottom respectively) for a star of effective temperature of 10^5 K.
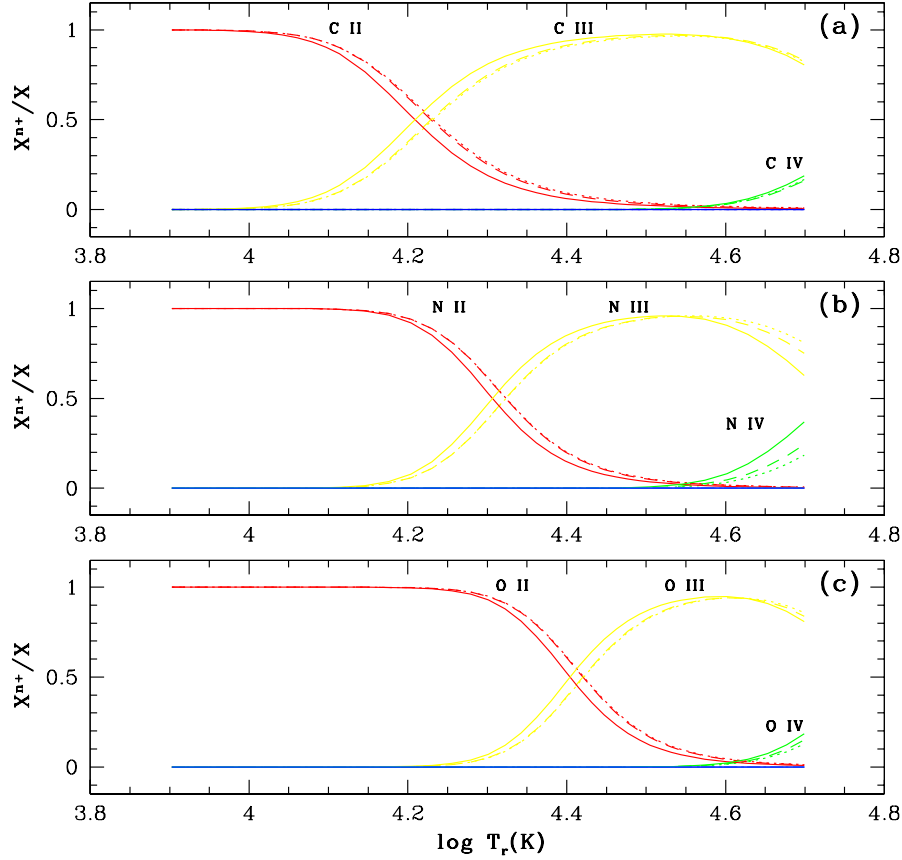
Fig. 5.— Ionization fractions for Carbon, Nitrogen, and Oxygen ions as a function of the radiation temperature T_r of the black body ionizing source: with new RAP cross sections from subroutine RESPHOT, and new unified recombination rates from subroutine RCRATE (solid lines), with new RAP cross sections and earlier recombination data as in CLOUDY (dashed lines), and with phototionization and recombination data as in CLOUDY (dotted lines); the calculations are for photon flux per cloud unit area of 10^{13} cm^{-2}, H density of 10^4 cm^{-3}, and electron temperature of 10^4 K. The curves show that the new unified recombination data for C,N,O leads to some significant differences in the ionization fractions.